Polymer 49 (2008) 2288–2297

Contents lists available at ScienceDirect

Polymer

journal homepage: www.elsevier.com/locate/polymer

Thermoplastic vulcanizates obtained by reaction-induced phase separation: Interplay between phase separation dynamics, final morphology and mechanical properties

Roy l'Abee [a,b], Han Goossens [a,b,*], Martin van Duin [a,c]

[a] Laboratory of Polymer Technology, Department of Chemical Engineering and Chemistry, Eindhoven University of Technology, P.O. Box 513, 5600 MB Eindhoven, The Netherlands
[b] Dutch Polymer Institute, P.O. Box 902, 5600 AX Eindhoven, The Netherlands
[c] DSM Research, P.O. Box 18, 6160 MD Geleen, The Netherlands

ARTICLE INFO

Article history:
Received 21 December 2007
Received in revised form 18 February 2008
Accepted 17 March 2008
Available online 21 March 2008

Keywords:
Morphology
Reaction-induced phase separation
Thermoplastic vulcanizates

ABSTRACT

Reaction-induced phase separation (RIPS) of miscible blends of poly(ε-caprolactone) (PCL) and an epoxy resin based on poly(propylene oxide) (PPO) was used to prepare thermoplastic vulcanizates (TPVs) with fine rubber dispersions. Scanning electron microscopy (SEM) confirmed the formation of cross-linked rubber particles dispersed in the thermoplastic matrix at PCL contents ≥20 wt%. The morphology development during phase separation was studied by optical microscopy (OM) and time-resolved small-angle light scattering (SALS). It was shown that higher curing temperatures lead to a decrease in rubber particle size, but at the same time lead to an increase in the extent of particle connectivity. In some cases, gelation of the PPO-rich phase limits full structure development, which leads to extensive connectivity between the dispersed rubber particles and a strong deterioration in tensile properties.

1. Introduction

Thermoplastic vulcanizates (TPVs) are blends consisting of a thermoplastic matrix and a cross-linked elastomer as the dispersed phase, leading to a unique combination of elastic properties and melt (re)processability [1,2]. TPVs are produced by a process known as dynamic vulcanization, in which the elastomer phase is selectively cross-linked during melt blending with the thermoplastic. The increasing viscosity of the elastomer phase during dynamic vulcanization affects the phase continuity by promoting phase inversion, which enables the cross-linked elastomer to become the dispersed phase. This process facilitates the dispersion of a large amount of cross-linked rubber into the thermoplastic matrix, which results in soft and highly elastic products. The physical properties of TPVs depend strongly on the blend composition, the cross-link density of the rubber phase and the rubber dispersion and particle size [1,2]. The strong dependence of the tensile properties on the rubber particle size was demonstrated by Coran and Araghi for TPVs based on poly(propylene) (PP) and ethylene–propylene–diene (EPDM) rubber [3,4]. Variation of the rubber particle size was accomplished by using pre-cross-linked EPDM milled to particles with different sizes [3] and by dynamic vulcanization at various shear rates [4]. Both the elongation at break and the tensile strength increased by a factor of five by decreasing the rubber particle size from 70 to 1 μm. Based on these results, it may be expected that TPVs with a sub-micron rubber dispersion have superior tensile properties compared to traditional TPVs.

Recently, a new approach for the preparation of TPVs was introduced with the potential of obtaining sub-micron rubber dispersions [5,6]. Phase separation of a miscible system based on a semi-crystalline thermoplastic polymer and an elastomer precursor was induced by selective cross-linking of the elastomer precursor. This method, which is known as reaction-induced phase separation (RIPS) or polymerization-induced phase separation (PIPS), can be applied to a wide variety of thermoplastic polymers in combination with an elastomer or a low-molar-mass elastomer precursor. Inoue et al. showed that TPVs can be prepared by dynamic vulcanization of miscible blends based on poly(vinylidene fluoride) (PVDF) and acrylic rubber (ACM) [5]. Dynamic vulcanization led to complex morphologies, since dispersion of both supra-micron and a small number of nano-sized ACM particles in a PVDF matrix were obtained, where well-developed PVDF crystalline lamellae were visible in the supra-micron ACM particles. Since miscible thermoplastic/elastomer blends are scarce due to their low gain in entropy upon mixing, the use of a low-molar-mass elastomer precursor in combination with a semi-crystalline

* Corresponding author. Laboratory of Polymer Technology, Department of Chemical Engineering and Chemistry, Eindhoven University of Technology, P.O. Box 513, 5600 MB Eindhoven, The Netherlands. Tel.: +31 40 2473899; fax: +31 40 2436999.
E-mail address: J.G.P.Goossens@tue.nl (H. Goossens).

0032-3861/$ – see front matter © 2008 Elsevier Ltd. All rights reserved.
doi:10.1016/j.polymer.2008.03.030

thermoplastic might be advantageous. Therefore, in this study miscible blends of poly(ε-caprolactone) (PCL) and an epoxy resin based on poly(propylene oxide) (PPO) were used as a model systems to study the potential of RIPS for the preparation of submicron TPVs [6].

The concept of RIPS based on miscible blends of epoxy resins and thermoplastic polymers has already been explored since the late 1960s and has successfully been applied in various industrial processes. RIPS has been proven to be useful for the toughening of brittle epoxy resins with rubbers [7–11] and thermoplastics [12–14] and for the processing of intractable polymers [15,16]. The miscibility and phase separation behavior [17–20] and crystallization kinetics [21,22] of PCL/epoxy systems have been studied in detail. However, all these studies deal with a thermoset matrix based on an aromatic epoxy resin with a high glass transition temperature (T_g), e.g. the diglycidyl ether of bisphenol-A (DGEBA). For these systems vitrification will occur, which drastically slows down the reaction and concurrent diffusional processes associated with phase separation. Although RIPS of miscible blends of thermoplastics and epoxy resins is said to be reasonably well understood, it is still a subject of in-depth studies because of the complexity that arises from the many parameters that influence the phase separation mechanism and the corresponding kinetics and, thus, the final morphology. The chemistry in miscible blends of thermoplastics and epoxy resins is complicated, since it involves chain extension, grafting and cross-linking, together with a redistribution of the reactive components during phase separation.

Preliminarily miscibility studies on the PCL/PPO system used for TPV production showed a clear melting temperature (T_m) depression of PCL as a function of the PPO concentration, which indicates miscibility of the mixture over the whole composition range at temperatures above T_m of PCL ($T_m = 60\ ^\circ C$) [6]. RIPS enabled the dispersion of up to 80 wt% of cross-linked PPO rubber in the thermoplastic PCL matrix. Fine rubber dispersions were obtained without applying blend compatibilization or dynamic shear forces during cross-linking. At high curing temperatures (T_{cure}) morphologies with a sub-micron rubber dispersion were obtained under quiescent conditions (static curing), while applying shear forces during the curing process (dynamic curing) led to significantly coarser morphologies. Extrapolation of the studies by Coran and Araghi [3,4] suggests that TPVs with a more refined rubber dispersion provide enhanced tensile properties. However, the dynamically-cured PCL/PPO-based TPVs showed a higher elongation at break and tensile strength than the statically-cured TPVs [6]. Based on electron microscopy studies, it was proposed that the somewhat disappointing tensile properties of the statically-cured TPVs are related to connectivity of the rubber particles. A similar observation was made by Ratna [23], who showed that rubber-toughened brittle epoxy resins prepared by RIPS initially demonstrate an enhancement of the toughness upon increasing T_{cure}, followed by a strong decrease in toughness upon a further increase of T_{cure}. Ratna proposed that at higher T_{cure} phase separation starts after the epoxy resin has formed a three-dimensional cross-linked network. Cross-linking of the epoxy resin induces diffusional restrictions, which limits the full development of a phase-separated morphology. Although no experimental proof was given, it is plausible that particle connectivity in reaction-induced phase-separated blends is related to coarsening and leads to deteriorated mechanical properties.

In this paper a more detailed study on the reaction-induced phase separation process of PCL/PPO systems is presented, which provides a better insight in the potential of RIPS for the preparation of (sub-micron) TPVs. Vitrification of the epoxy resin does not occur, since the fully cured PPO/TETA system has a T_g below room temperature. The curing reaction of PPO, both neat and in the blends with PCL, is studied by Fourier transform infrared (FTIR) spectroscopy. Optical microscopy (OM) and scanning electron microscopy (SEM) are used to study the later stages of RIPS and the final morphology, respectively, whereas small-angle light scattering (SALS) is used to study the phase separation dynamics. Finally, the morphology development during RIPS is related to the tensile properties of the TPVs.

2. Experimental

2.1. Materials

Poly(ε-caprolactone) (PCL, $M_n = 20$ kg/mol, $M_w = 37$ kg/mol) was kindly supplied by Solvay Caprolactones, UK. Liquid poly(propylene oxide)-based epoxy resin (PPO, Aldrich) having a propylene oxide block length of 5 and an epoxy equivalent weight (EEW) of 190 g/eq, was used. Triethylene tetramine (TETA) having an amine hydrogen equivalent weight (AEW) of 27 g/eq was used as the curing agent and was kindly supplied by Huntsman (Fig. 1).

2.2. Blend preparation

Homogeneous blends were prepared by dissolving PCL in the liquid PPO at temperatures above 70 °C in a round bottom flask. The curing agent was added to the solution under continuous stirring at 250 rpm until a homogeneous mixture was obtained, after which the stirring was stopped during the remainder of the experiment. TETA was used in stoichiometric epoxy/amine ratios. Curing temperatures ranged from 80 to 160 °C.

2.3. Characterization

2.3.1. Fourier transform infrared (FTIR) spectroscopy

The curing reaction of PPO, both neat and in the blends with PCL, was studied by FTIR spectroscopy. Spectra were obtained by placing (PCL/)PPO/TETA blends on the diamond crystal of a Specac Golden Gate attenuated total reflection (ATR) setup placed in a BioRad Excalibur 3000 spectrometer. Fifty spectra at a resolution of 4 cm^{-1} over a spectral range of 600–5000 cm^{-1} were signal-averaged and the resulting spectra were analyzed using the BioRad Merlin 3.0 software. The intensity of the absorption band assigned to the symmetric ring deformation of the epoxy group at 843 cm^{-1} (A) was used to calculate the epoxy conversion (α) by the following equation:

$$\alpha = \frac{A_0 - A_t}{A_0 - A_\infty} \tag{1}$$

where A_0 and A_∞ represent the initial and final intensities, respectively, while A_t represents the intensity at curing time t. The anti-symmetric C–O–C stretching vibration of the propylene oxide repeat unit at 1069 cm^{-1} was used as reference peak to correct for changes in the penetration depth of the evanescent wave, which is approximately 1 μm. For the PCL/PPO blends, the spectrum of amorphous, molten PCL was subtracted to obtain the spectra of PPO.

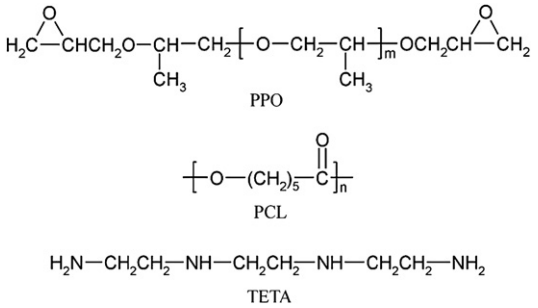

Fig. 1. Chemical structures of PPO, PCL and TETA.

2.3.2. Optical microscopy (OM)

The phase separation process upon curing was studied by optical microscopy using a Zeiss Axioplan 2 microscope equipped with a Zeiss Axiocam camera. The images were analyzed with the accompanying AxioVision v3.0.6 software. Samples were sandwiched between two thin glass slides and fixed on a Linkam THMS-600 hot-stage for temperature control.

2.3.3. Scanning electron microscopy (SEM)

Morphological investigations were performed with a scanning electron microscope (SEM) (model XL30 FEG, FEI) at an acceleration voltage of 10 kV. The fully cured samples were fractured in liquid nitrogen and the fractured surfaces were etched with tetrahydrofuran (THF) in order to remove all soluble PCL. After drying overnight under vacuum, the samples were sputter-coated with a thin layer of gold to improve the electrical conductivity.

2.3.4. Small-angle light scattering (SALS)

The phase separation dynamics were studied by small-angle light scattering (SALS). A 1 mW-intensity stabilized He–Ne laser was used as incident light source. The light was guided through a pinhole and then through the sample, which was fixed between two glass slides. The temperature was controlled by a Linkam THMS-600 hot-stage. The scattered light was projected on a semi-transparent poly(propylene) screen. The scattering patterns were captured with a 16-bit 512 × 512-CCD camera (Versarray:512B Princeton CCD with a ST-133 controller), equipped with a Rodenstock Rodagon 50 mm f 1:2.8 lens with a variable focal distance. The CCD camera was linked to a personal computer for data acquisition and analysis. The scattering angles were calibrated with a 300 lines/mm grid. The data acquisition time was typically 1000 ms per image and was controlled by a home-made script running under V++ for Windows (version 4.0, Digital Optics Ltd) [24].

2.3.5. Tensile tests

Films with a thickness of 1 mm were compression molded at 100 °C at 100 bar from which dumbbell-shaped tensile bars (32 × 2 × 1 mm) were punched. Tensile tests were performed at 0.2 mm/s using a 2.5 kN force cell on a Zwick Z010 tensile tester according to ASTM D412. The equipment was controlled with TestXpert v7.11 software. Each sample was tested in at least 10-fold.

3. Results and discussion

3.1. PPO/TETA reaction

First, the reaction kinetics of the neat PPO cured with TETA as measured by FTIR spectroscopy are discussed, after which the influence of PCL on the reaction kinetics in the miscible blends will be addressed. Fig. 2 shows that the conversion rate of the neat PPO increases with increasing T_{cure}. The final epoxy conversion is only slightly influenced by T_{cure} and is almost complete (>95%). Auto-catalytic effects, which arise from the formation of hydroxyl groups during the curing process, are commonly observed for epoxy/amine reactions and are characterized by S-shaped conversion-versus-time profiles [25,26]. However, such auto-catalytic effects seem to be absent in our systems (Fig. 2). This may be attributed to the fast reaction kinetics, which makes it difficult to determine the starting point of the reaction accurately. The activation energy (E_α) of the curing reaction was calculated by evaluating the slope of the plot of $\ln(t_\alpha)$ against $1/T$, where t_α is the time t required to reach a specific epoxy conversion α at an isothermal curing temperature T_{cure} [27]. The calculated E_α ranges from 68 to 79 kJ/mol for conversions ranging from 40 to 80%. The dependency of E_α on α is a well-known phenomenon in epoxy/amine reactions and is generally attributed to the multi-step reaction mechanism that results in complex kinetics [27,28].

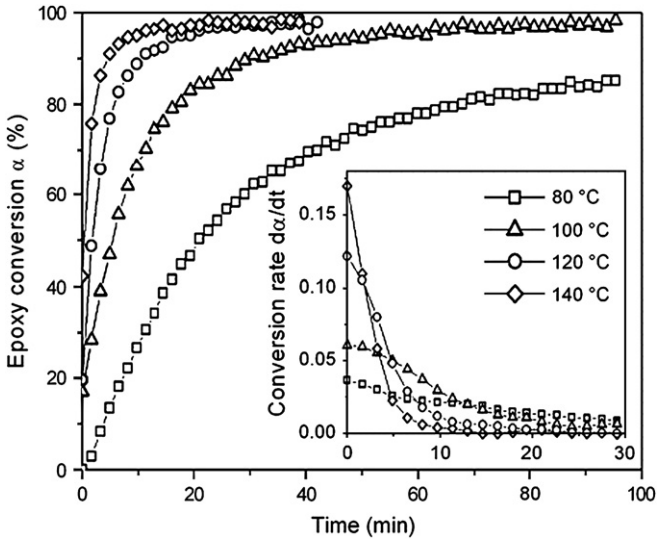

Fig. 2. Epoxy conversion upon curing of the neat PPO as measured by FTIR spectroscopy. The inset shows the conversion rate as a function of time.

Fig. 3 shows that the addition of 50 wt% PCL to PPO slows down the initial conversion rate. The concentration of the reactive epoxy and amine groups is decreased by the addition of PCL, which decreases the probability of the epoxy/amine reaction to occur. Fig. 3 shows that the final epoxy conversion is somewhat decreased by the addition of PCL. Previous studies on blends of thermoplastic polymers with aromatic epoxy resins showed that the addition of 20–40 wt% of thermoplastic polymer decreased the final epoxy conversion from >95% down to 60% [29,30]. This significant decrease in final epoxy conversion was attributed to vitrification of the system, occurring when T_g of the partially reacted epoxy resin becomes equal to T_{cure}. Since the PPO/TETA system used in this study has a T_g of 5 °C after full conversion, vitrification of the system does not occur. The rubber gel content of the blends was measured by extraction with THF, which dissolves PCL and non-cross-linked PPO. A decrease in the rubber gel content was observed upon increasing the PCL concentration, which is consistent with the FTIR

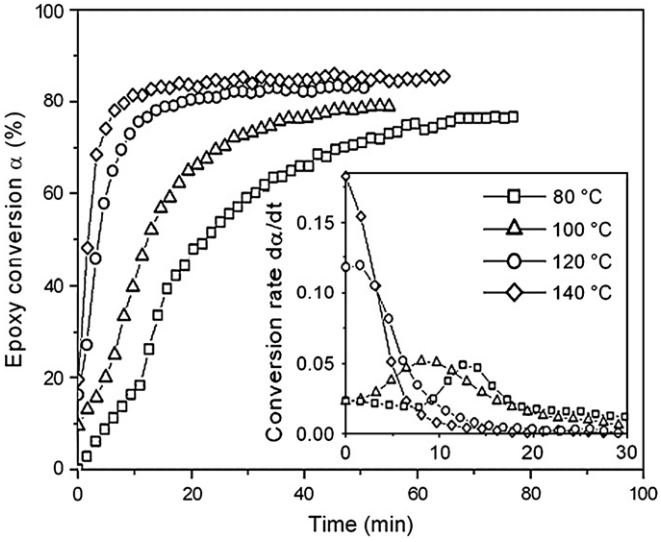

Fig. 3. Epoxy conversion upon curing of PPO in a PCL/PPO mixture containing 50 wt% PCL as measured by FTIR spectroscopy. The inset shows the conversion rate as a function of time.

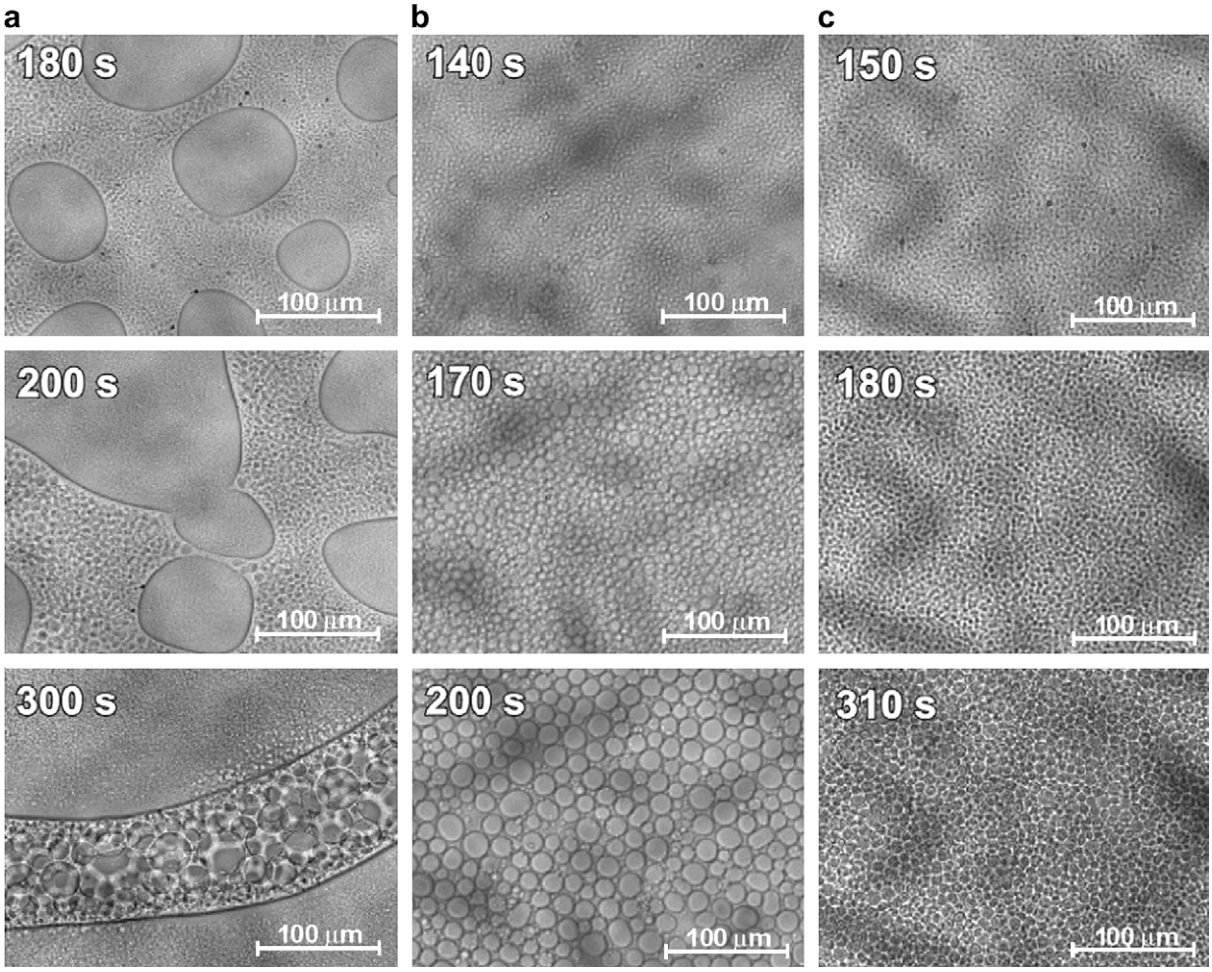

Fig. 4. OM images of PCL/PPO blends cured at 100 °C containing (a) 10 wt% PCL; (b) 20 wt% PCL and (c) 30 wt% PCL. The curing times are given in the left top corner of each image.

measurements. The gel content appeared to be fairly constant over a range of T_{cure} from 80 to 160 °C. FTIR spectroscopy showed that a small amount of PCL (typically in the range of 1–2 wt%) could not be extracted from the blends [6]. The decrease in final epoxy conversion in the PCL/PPO system can be explained by a redistribution of the amine curing agent over the PPO and PCL phases after phase separation, as a result of which part of the amine is no longer available for the cross-linking reaction [30]. Partial amidation of PCL with the amine will also lead to a lower final epoxy conversion and to grafting of PCL onto the epoxy network. Previous studies showed that the hydroxyl end groups of PCL might react with the oxirane rings of the epoxy resin, which lead to grafting of PCL chains onto the cross-linked particles [17]. Additionally, traces of water in the system may lead to partial hydrolysis of PCL under the formation of hydroxyl and carboxylic acid end groups. The carboxylic acid end groups readily react with the oxirane rings of the epoxy resin. The latter reaction is most likely responsible for the grafting.

In contrast to the neat PPO, which shows a continuous decrease in conversion rate as a function of time (inset of Fig. 2), the PCL/PPO blends show a distinct maximum in the conversion rate (inset of Fig. 3), which shifts to shorter reaction times upon increasing T_{cure}. The acceleration of the conversion rate is not related to an autocatalytic effect, but can be explained by phase separation of the PCL/PPO blends during curing, as will be discussed in the next section. The reaction time at which the conversion rate shows a maximum value is close to the onset of phase separation as determined by SALS (Fig. 8). As stated earlier, the presence of PCL in the blend decreases the local concentration of epoxy and amine groups, thereby decreasing the conversion rate. After phase separation, PPO-rich and PCL-rich phases are formed. In the PPO-rich phase the epoxy concentration is higher than before phase separation, which increases the conversion rate [31]. When T_{cure} is increased, phase separation sets in earlier (Fig. 8) and, concomitantly, the maximum in conversion rate shifts towards shorter curing times.

The molar mass build-up of the reacting PPO/TETA system can be calculated by the statistical model derived by Macosko and Miller [32,33]. Given the functionalities of PPO and TETA and their molar ratio, the gel point, defined as the increase in weight-average molar mass (M_w) to infinity, is reached at an epoxy conversion of 50%. Based on this calculation, the reaction time at which the gel point is reached can be estimated from the presented FTIR spectroscopy results, both for the neat PPO and for PPO in blends with PCL. This information will be used in a later section, where the phase separation process of the blends is related to the final morphology.

3.2. Morphology development

To determine suitable PCL/PPO compositions for the preparation of TPV morphologies (i.e. cross-linked PPO rubber particles dispersed in the PCL matrix), first the late stages of the phase separation process and the morphologies after full curing are studied by OM and SEM, respectively. Based on the OM and SEM results, the earlier stages of the phase separation process of several relevant compositions are studied in more detail by SALS. Fig. 4a shows the

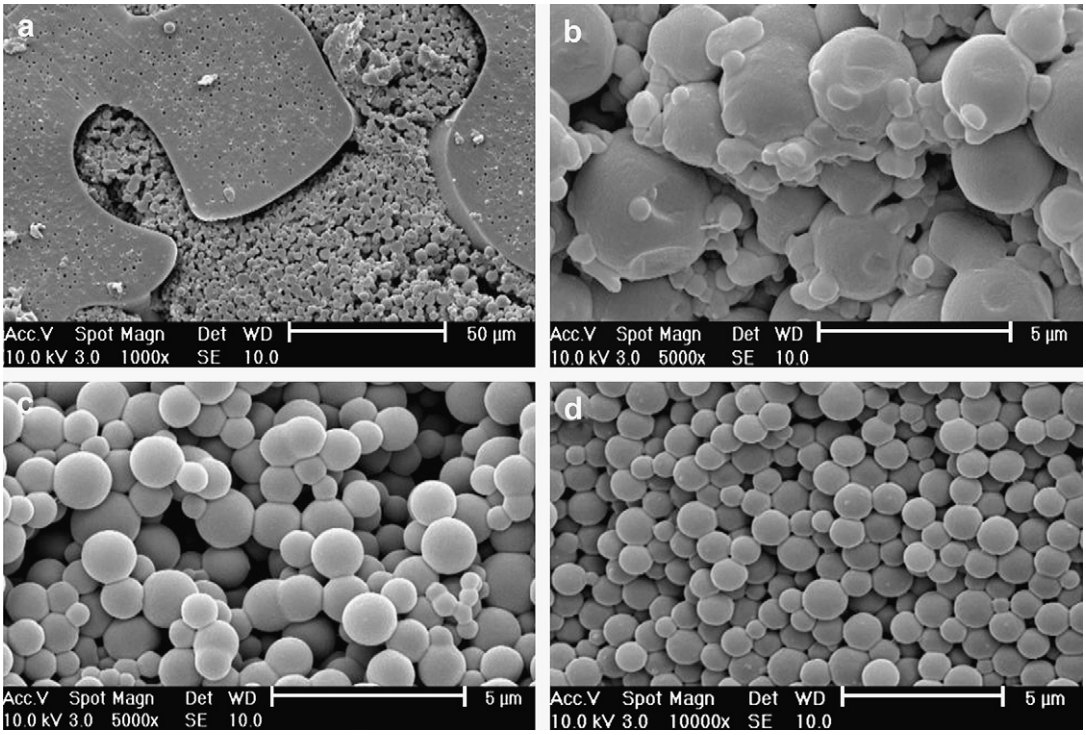

Fig. 5. SEM images of PCL/PPO blends containing (a) 10 wt% PCL; (b) 20 wt% PCL; (c) 40 wt% PCL and (d) 60 wt% PCL after full curing at 140 °C.

structure development of a PCL/PPO blend containing 10 wt% PCL. At the time that phase separation is detectable, relatively large co-continuous structures are observed, which further coarsen with time. This indicates that the composition of 10 wt% PCL is close to the critical composition and that phase separation occurs via spinodal decomposition (SD). Small sub-inclusions are observed in both phases, which indicate the occurrence of secondary phase separation. Comparison of the OM image of Fig. 4a at 300 s with the corresponding SEM micrograph of the same sample (Fig. 5a) allows for identification of the larger inclusions (average diameter $\overline{D} \sim 10$ μm) as PPO-rich droplets that develop in the PCL-rich phase, whereas the smaller inclusions ($\overline{D} \sim 1$ μm) are identified as PCL-rich droplets formed in the PPO-rich phase.

Compositions with PCL contents of 20 and 30 wt%, i.e. positioned further away from the critical composition, show a different morphology development with time (Fig. 4b and c, respectively). In these systems, phase-separated structures are spontaneously formed on a relatively small scale. These structures rapidly grow in size to form spherical particles having $\overline{D} \sim 10$–15 μm for 20 wt% PCL and $\overline{D} \sim 3$–7 μm for 30 wt% PCL. A similar structure development is found at PCL contents of 40 and 50 wt%, although the structural dimensions decrease. Fig. 5 confirms that TPV morphologies are formed at PCL contents ≥20 wt% and that the rubber particle size decreases with increasing PCL content.

Based on OM and SALS experiments, Vanden Poel et al. reported that the phase separation process for miscible blends of PCL with an aromatic epoxy resin with off-critical compositions occurs via the formation of a bi-continuous structure, which breaks up into spherical particles [20]. The formation of bi-continuous structures was not observed for the PCL/PPO systems, which implies that the formation of a bi-continuous structure and its subsequent break up into spherical particles occurs rapidly and at a relatively small scale. Since the OM and SEM studies show that no typical TPV morphologies are obtained at PCL contents below 20 wt%, the remainder of this paper will only discuss blends with PCL contents of 20 wt% and higher.

Fig. 6 shows SEM images of fully cured PCL/PPO blends containing 60 wt% PCL. Clearly, T_{cure} has a significant influence on the final morphology. Spherical rubber particles with little connectivity are obtained at low T_{cure} (80 °C, Fig. 6a), whereas a higher T_{cure} (140 °C, Fig. 6b) leads to extensive particle connectivity. This

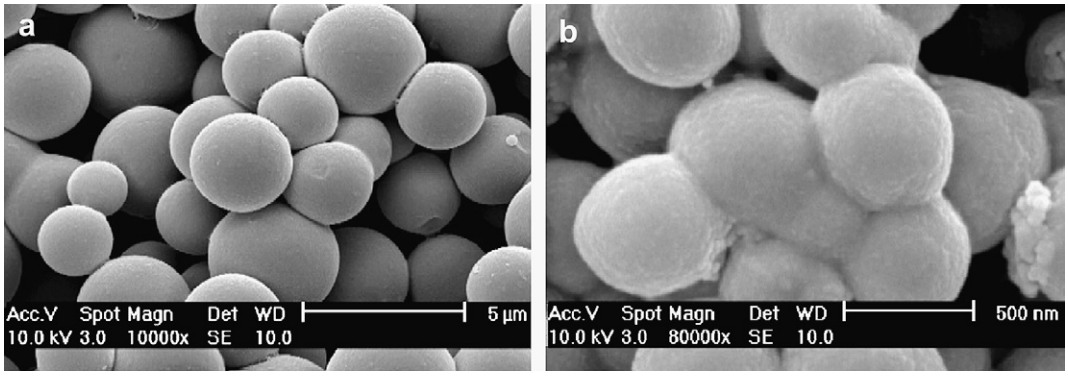

Fig. 6. SEM images of PCL/PPO blends containing 60 wt% PCL after full curing at (a) 80 °C and (b) 140 °C. The PCL phase was extracted with THF, so only the cross-linked rubber phase is visible.

phenomenon was previously discussed by Yamanaka and Inoue, who introduced the so-called connected-globule structure for RIPS of miscible blends of poly(ether sulphone) (PES) and an aromatic epoxy resin [34]. They proposed that, after a periodic increase of the bi-continuous structure formed by SD, the phase connectivity is disrupted by an increase in interfacial tension, eventually leading to a dispersed droplet-like morphology. A connected-globule structure is formed when complete break up of the co-continuous structure cannot be realized, e.g. by gelation or vitrification of the epoxy-rich phase. However, since phase separation of the PES/aromatic epoxy resin was affected by both gelation and vitrification, the main origin of particle connectivity could not fully be clarified.

3.3. Phase separation dynamics

To study the structure development during the early stages of phase separation, light scattering studies were performed on the PCL/PPO blends during curing. Fig. 7 shows the evolution of the SALS patterns of a PCL/PPO blend containing 30 wt% PCL upon curing at 100 °C. Typically, no appreciable light scattering is detected for the homogeneous blend during the early stages of the reaction. After ~4 min, a maximum in the scattering pattern appears at a certain scattering vector q_{max}, where q is the scattering vector ($q = (4\pi/\lambda)\sin(\theta/2)$ where λ is the wavelength and θ is the scattering angle), indicating the development of a well-correlated, phase-separated structure. Upon further curing, q_{max} shifts to lower values with increasing maximum intensity (I_{max}), which implies coarsening of the phase-separated structure (arrow 1 in Fig. 7). These changes in the scattering profile are typical for the later stages of spinodal decomposition (SD) [35–37]. Similar scattering profiles were obtained at PCL contents ranging from 20 to 50 wt% PCL and T_{cure} from 80 to 140 °C. These results suggest that RIPS of the PCL/PPO blends proceeds via reaction-induced spinodal decomposition. Since a highly reactive, six-functional curing agent is used (TETA), the curing reaction is expected to proceed fast compared to phase separation. This implies that phase separation via nucleation and growth (NG) is suppressed and, therefore, SD is indeed the most likely phase separation mechanism to be observed [38]. Yamanaka et al. actually stated that RIPS can only proceed via SD, since the NG process is too slow to occur [37,39]. Although this statement is only true for systems with a relatively high interfacial tension (the free energy barrier for nucleation is proportional to the third power of the interfacial tension), SD is generally accepted as the most common phase separation process for RIPS of miscible blends of epoxy resins and thermoplastics [10,40]. Due to the high reaction rate of the PPO/TETA system, the early stages of the SD process, which is characterized by an increasing intensity at a constant q_{max}, cannot be observed here [35].

Fig. 7 shows that after a curing time of ~6 min, a shoulder appears next to the low-angle scattering peak (arrow 2). The position of the shoulder suggests that a structure with a characteristic length scale of 2–3 μm appears in addition to the 4–8 μm-sized structure formed during the initial stages of phase separation. Vanden Poel et al. observed a similar scattering profile for off-critical mixtures of PCL and an aromatic epoxy resin [20]. They assigned the appearance of the wide-angle peak to break up of the earlier developed structure into smaller particles. This explanation is also plausible for the shoulder in the scattering profile shown in Fig. 7. Since the size of the newly formed particles is relatively small (2–3 μm), they are not clearly visible in the OM images presented in Fig. 4c. A similar phase separation behavior was observed for this blend composition at all curing temperatures studied. At higher PCL contents the occurrence of the wide-angle shoulder next to the low-angle peak was not observed.

Some authors [20,35] reported that the phase separation process in miscible blends of PCL and aromatic epoxy resins changes from SD to NG upon increasing the PCL content. This is due to the decrease in curing rate in the presence of PCL and to a widening of the metastable region upon deviation from the critical point. In the case of PCL/PPO blends cured with TETA, such a transition from SD to NG upon increasing the PCL content is not observed; SD is the dominating phase separation mechanism up to 50 wt% PCL. As discussed earlier, the absence of NG can be attributed to the relatively high reaction rate of the PPO/TETA reaction [37–39].

The onset of phase separation during isothermal curing of the PCL/PPO mixtures is identified by SALS as the first increase of the scattered intensity (Fig. 8). Phase separation sets in earlier with increasing T_{cure} and decreasing PCL content. At very low PCL contents the onset of phase separation should go to infinite values (dotted lines), since the neat PPO will not phase separate.

The growth dynamics in the intermediate and late stages of SD is often described by a power-law relation [36,41,42]:

$$q_{max}(t) \propto t^{-\alpha} \tag{2}$$

$$I_{max}(t) \propto t^{\beta} \tag{3}$$

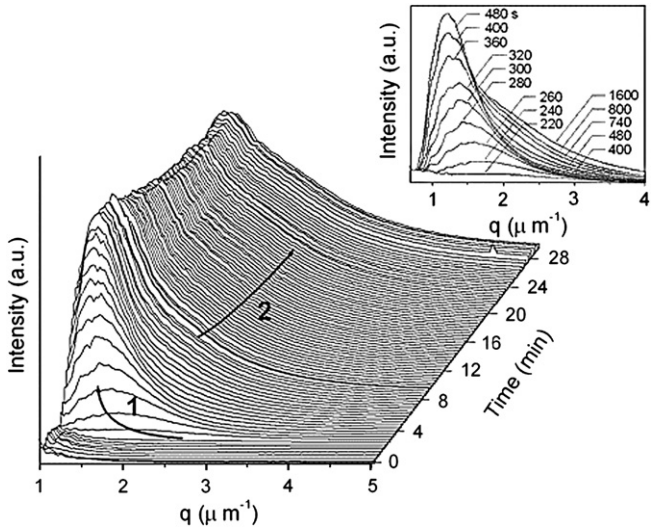

Fig. 7. Time-resolved evolution of the SALS pattern of a PCL/PPO mixture with 30 wt% PCL cured at 100 °C.

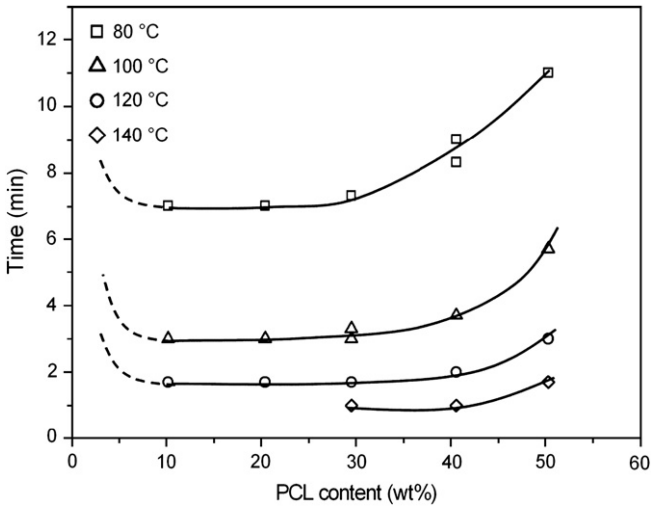

Fig. 8. Onset of phase separation for PCL/PPO blends at various T_{cure} as determined by SALS.

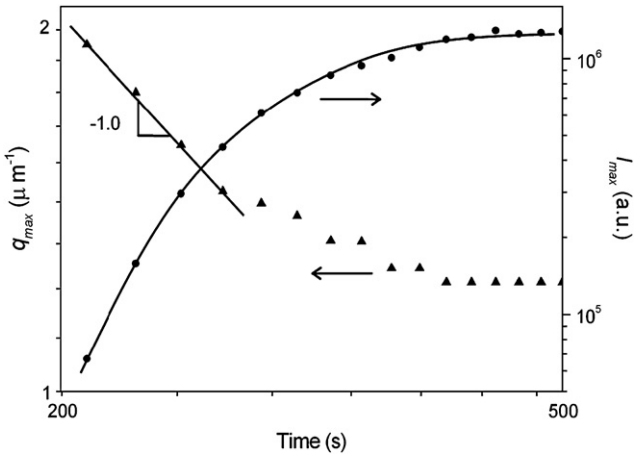

Fig. 9. Variation of q_{max} and I_{max} with time of a PCL/PPO mixture with 30 wt% PCL upon curing at 100 °C.

The experimental data of Fig. 7 for off-critical PCL/PPO blends can be translated to the variation of q_{max} and I_{max} with time as shown in Fig. 9. The maximum of the scattering vector q_{max} fits the power-law expression only at the early stages of phase separation. The power-law coefficient α is equal to 1.0, indicating that the coarsening process is hydrodynamically controlled [43]. The maximum peak intensity does not follow a power-law over any reasonable time interval. This may be attributed to the occurrence of apparent phase dissolution, which originates from the relatively large change in refractive index of the PPO phase upon reaction with TETA. As the curing reaction proceeds, the refractive index of the PPO-rich phase becomes close to that of the PCL-rich phase and the total scattered intensity decreases [16,44].

The $\log(q_{max})$ versus $\log(t)$ plots obtained at various T_{cure} can be superimposed by horizontal and vertical shifting to form a single mastercurve, with a_T the horizontal and b_T the vertical shift factor. This suggests that the time–temperature superposition (TTS) principle is valid. Fig. 10 shows the result of TTS of q_{max} to a reference temperature (T_r) of 80 °C for the 30 and 50 wt% PCL blends. The power-law coefficient α equals 1.0 for both the blends over the whole range of T_{cure} (80–140 °C), which indicates similar phase separation dynamics. The inset of Fig. 10 gives plots of $1/\log(a_T)$

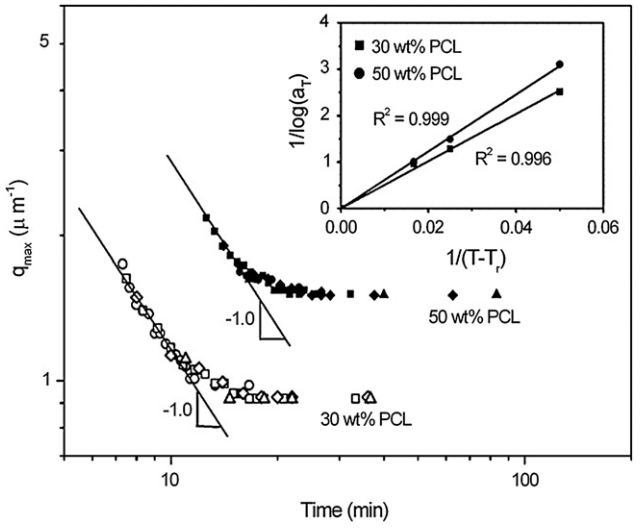

Fig. 10. Mastercurves of q_{max} versus time of PCL/PPO blends with 30 and 50 wt% PCL during curing at 80, 100, 120 and 140 °C. The curves are superimposed to a reference temperature (T_r) of 80 °C. The inset shows the relationship between the horizontal shift factor a_T and the relative temperature $T - T_r$.

against $1/(T - T_r)$, which follow a linear relationship. This demonstrates that a Williams–Landel–Ferry (WLF)-like function, which is typically applied to describe the relaxation time of amorphous polymers controlled by the diffusion of segments [26,45], is valid. The TTS principle is also applicable to the $\log(I_{max})$ versus $\log(t)$ plots obtained at various T_{cure}. Mastercurves were obtained by using similar values for a_T as were used for TTS of the $\log(q_{max})$ versus $\log(t)$ plots. The observation that the late-stage SD process obeys the TTS principle and can be described by the WLF-equation suggests that the coarsening process is mainly controlled by viscoelastic flow [42].

It was previously reported by Tanaka that viscoelastic phase separation is a universal phenomenon common to all dynamic asymmetrical mixtures [46,47]. The dynamic asymmetry can originate from the difference in size of the component molecules or the existence of specific transitions, such as T_g [48,49]. Viscoelastic phase separation is characterized by changes of the relevant coarsening mode in time; namely, it switches from an initial diffusive mode to an elastic mode and eventually to a hydrodynamic mode. In the elastic regime, the elastic force balance determines the morphology instead of the interfacial tension. Therefore, fixation of the morphology in the elastic regime (e.g. by gelation or vitrification) leads to connectivity between the PPO domains and to a co-continuous morphology in the extreme case. When the reaction is sufficiently slow, the coarsening process can proceed further into the hydrodynamic regime. In that case the interfacial energy overcomes the elastic energy and the PPO domains change from an anisotropic to a spherical shape. The occurrence of rubber connectivity in our PCL/PPO blends, as observed in Fig. 6b, can be explained by a shift in structure fixation by gelation from the hydrodynamic to the elastic regime with increasing T_{cure}.

The scattering vector is related to the characteristic length scale (l_c) by $l_c = 2\pi/q_{max}$, where l_c corresponds to the distance between similar phases, separated by the other phase and measured from centre to centre. The development of l_c at various T_{cure} is shown for blends containing 30 and 50 wt% PCL in Fig. 11a and b, respectively. During the first stages of phase separation l_c increases with time, but eventually levels off, which indicates that further structure development is suppressed. An increase in T_{cure} leads to a decrease in l_c, which is consistent with the SEM results presented in earlier work [6]. The arrows shown in Fig. 11 indicate the curing times at which gelation sets in. As discussed in the section on the PPO/TETA reaction, the gel points are calculated from FTIR spectroscopy results by using the model proposed by Macosko and Miller. It has been shown that the calculated gel point agrees very well with the experimentally determined gel point, both for neat epoxy/amine systems as well as for their miscible blends with thermoplastic polymers [50]. Nevertheless, the position of the gel point should be used with care, since it is based on the combination of experimental and statistical data.

Fig. 11a shows that for blends with a PCL content of 30 wt%, l_c levels off prior to reaching the gel point. This implies that structure coarsening can proceed up to the hydrodynamic regime, where a decrease in interfacial energy leads to the formation of spherical PPO domains dispersed in the PCL matrix. For blends containing 50 wt% PCL, l_c levels off abruptly after reaching the gel point, which is most profound at high T_{cure} (Fig. 11b). This suggests that the phase separation process is hindered by gelation of the PPO-rich phase, thus influencing the final morphology. Under these conditions, the viscoelastic domain formation may not switch to the hydrodynamic regime and fixation of the morphology shifts towards the elastic regime, leading to the formation of a connected-globule structure as shown in Fig. 6b.

Fig. 12 combines the results from the onset of phase separation (Fig. 8) with the FTIR spectroscopy data on the extent of the epoxy conversion during curing (Figs. 2 and 3). The T_m depression curve is

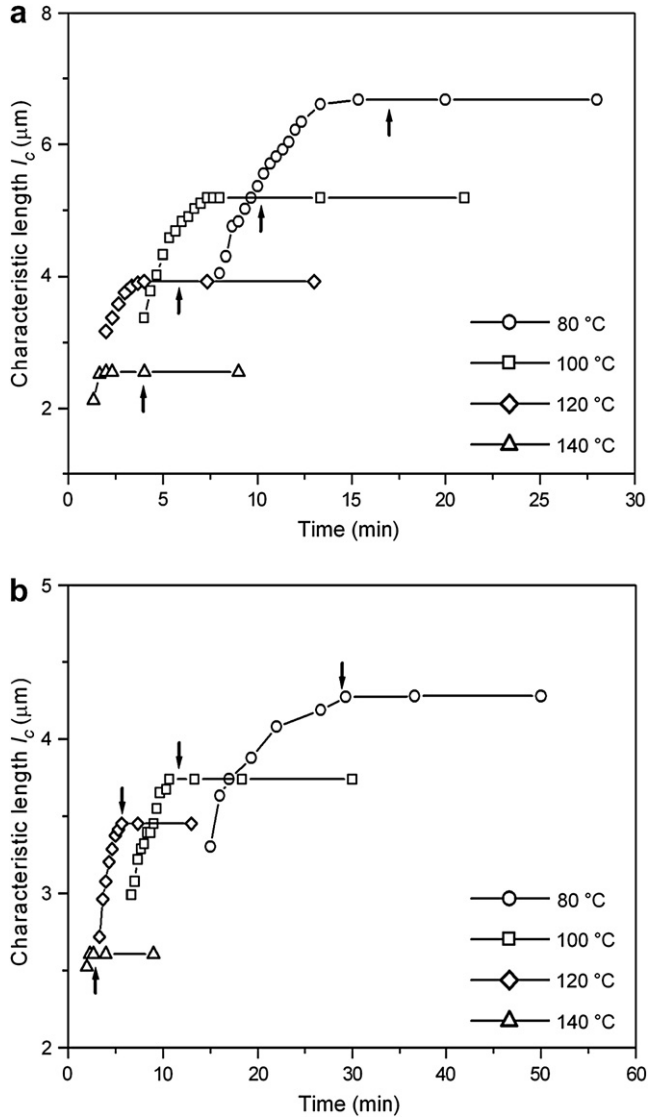

Fig. 11. Variation of l_c with T_{cure} for PCL/PPO blends containing (a) 30 wt% PCL and (b) 50 wt% PCL. The arrows indicate the position of the gel point.

represented by an epoxy conversion (α) of 0%. Phase separation sets in at higher α upon increasing the temperature, which indicates that the system is more miscible at higher temperature. From Fig. 12 it is evident that the phase separation of PCL/PPO blends with relatively high PCL contents at high T_{cure} is interfered by gelation, which leads to extensive particle connectivity (Fig. 6b). Such particle connectivity is not expected for PCL/PPO blends with 40 wt% PCL, since phase separation typically occurs prior to gelation. However, increasing T_{cure} leads to an increase in quench rate, i.e. an increase in thermodynamic quench depth with time, which suppresses structure coarsening prior to reaching the gel point of the system [36]. Consequently, one may generally expect a morphology with smaller particles and an increasing extent of particle connectivity upon increasing T_{cure}.

3.4. Correlation between morphology and properties

Only the tensile properties of PCL/PPO blends containing 40 and 60 wt% PCL will be discussed, since they are the most representative for TPVs. Samples with higher PCL contents exhibit a high modulus and poor elastic behavior and samples with lower PCL

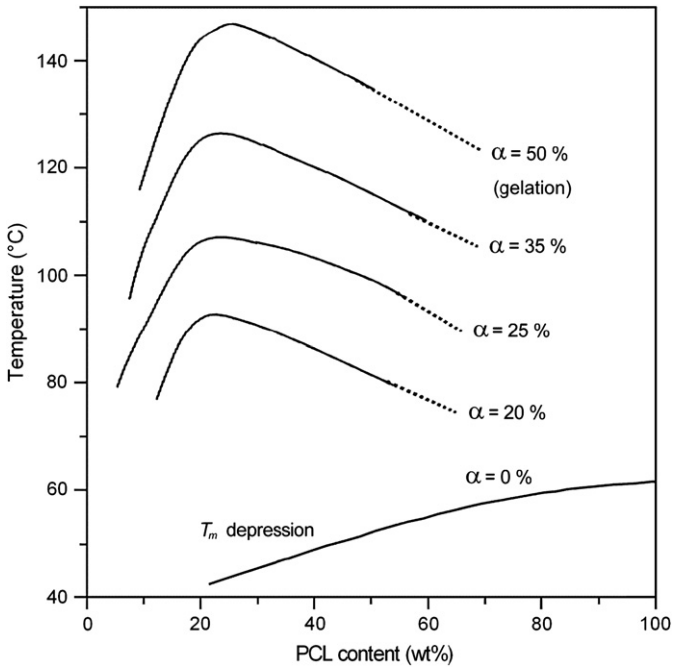

Fig. 12. Epoxy conversion (α) at the onset of phase separation of PCL/PPO blends. Each line represents the onset of phase separation at the indicated α.

contents lead to co-continuous morphologies and, thus, can hardly be melt processed.

Fig. 13 shows the tensile properties of PCL/PPO blends containing 40 wt% PCL cured at various temperatures. The rubber particle size decreases from 3.0 to 0.9 μm when T_{cure} is increased from 80 to 160 °C. A decrease in tensile modulus, elongation at break and tensile strength is observed with decreasing rubber particle size, which is in contrast to the studies of Coran [3] and Araghi [4] on PP/EPDM TPVs. This deterioration in tensile properties might be explained by various structural changes of the TPV, such as variations in the crystallinity of PCL, degradation of the PCL phase, different cross-link densities of the PPO rubber phase, incomplete phase separation and/or changes in the morphology. Variations in the crystallinity of the PCL phase were not observed; all samples showed a crystallinity of 47% as measured by DSC during the second heating run. Degradation of the PCL phase was also not observed; all samples, including the neat PCL, had M_n of 20 kg/mol and M_w of 38 kg/mol as measured by size exclusion chromatography (SEC) on the THF-extract of the blends. DSC showed the presence of two T_gs at −55 °C and at 5 °C for all samples,

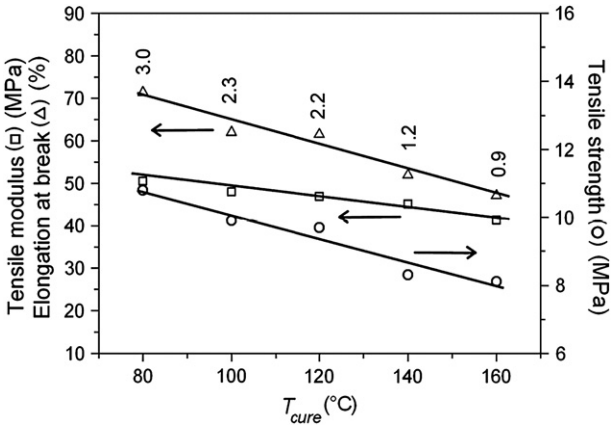

Fig. 13. The effect of T_{cure} on tensile properties for PCL/PPO blends containing 40 wt% PCL. The rubber particle size is indicated in the figure.

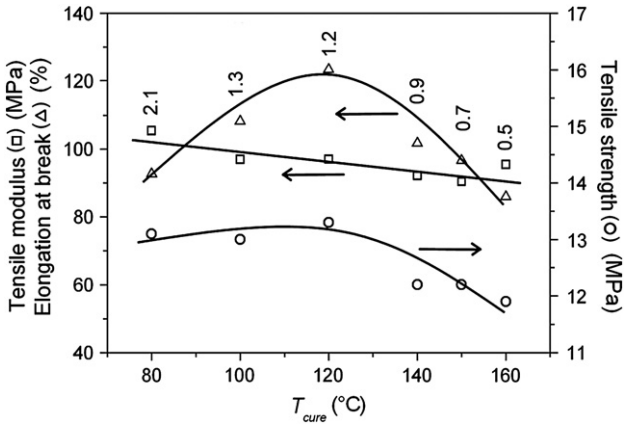

Fig. 14. The effect of T_{cure} on tensile properties for PCL/PPO blends containing 60 wt% PCL. The rubber particle size is indicated in the figure.

assigned to the PCL phase and the cross-linked PPO phase, respectively. The constant T_g for the cross-linked PPO phase indicates that the cross-link density in all samples is the same. In addition, complete phase separation has occurred, since the observed T_gs are equal to the T_gs of the pure components. The small differences in gel content and in the amount of grafted PCL as discussed in Section 3.1 cannot fully account for the differences in tensile properties as shown in Fig. 13. It can therefore be concluded that partial connectivity of the rubber particles, which increases with T_{cure} as discussed in detail in the previous section, causes the deterioration in tensile properties. Connection of the rubber particles causes the morphology to shift from a dispersed droplet-like structure towards a co-continuous structure. Consequently, the influence of the soft, cross-linked PPO phase on the tensile properties increases. Since the tensile modulus of the cross-linked PPO is much lower (~2 MPa) than the tensile modulus of PCL (~280 MPa), interconnection of the PPO particles will decrease the modulus of the TPV. Similarly, the elongation at break and the tensile strength of the cross-linked PPO are lower than those of PCL, which explains the decrease in elongation at break and tensile strength of the TPVs. By increasing T_{cure} not only the rubber particle size is decreased, but also the connectivity increases. As a result, the positive effect of the particle size reduction on the tensile properties seems to be counteracted by the negative effect of the rubber connectivity.

PCL/PPO-based TPVs containing 60 wt% PCL show two different regimes for the tensile properties (Fig. 14). The elongation at break and the tensile strength are somewhat improved upon increasing T_{cure} from 80 to 120 °C, which may be attributed to the decrease in rubber particle size. However, at $T_{cure} \geq 140$ °C a significant drop in the tensile properties is observed. For the TPVs containing 60 wt% PCL, a clear range of T_{cure} exists where gelation of the PPO phase interferes with the phase separation process, i.e. at $T_{cure} \geq 140$ °C (Fig. 12). These blends experience significant hindrance of the phase separation process, leading to a high extent of rubber connectivity (Fig. 6b) and, consequently, to a significant deterioration in tensile properties. Conversely, applying lower T_{cure} allows for a full development of the phase-separated structure with only little rubber connectivity (Fig. 6a).

4. Conclusions

RIPS of miscible PCL/PPO blends was used to prepare (sub-micron) TPVs with up to 80 wt% of cross-linked PPO rubber dispersed in the PCL matrix [6]. OM and SALS studies indicate that phase separation of PCL/PPO blends with a composition ranging from 10 to 50 wt% PCL is dominated by SD. Within the applied temperature region, the phase separation behavior follows the TTS principle. The growth-dynamics of the PPO droplets can be described by the WLF-equation, which suggests that the coarsening process is mainly controlled by viscoelastic flow. At relatively low PCL contents, coarsening proceeds into the hydrodynamic regime, which leads to the formation of spherical rubber particles that are slightly connected to each other. The particle connectivity increases with T_{cure}. At relatively high PCL contents, an increase in T_{cure} leads to fixation of the morphology in the elastic regime. This explains the extensive particle connectivity as observed by SEM and the consequent deterioration in tensile properties. Fixation of the morphology is fully determined by gelation of the PPO-rich phase, since vitrification of the PPO-rich phase does not occur in this system. The formation of a connected-globule structure might be prevented by using a less functional curing agent or by applying a dynamic curing process [6]. Unfortunately, these suggestions to prevent rubber connectivity will result in an increase of the rubber particle size, which is expected to lead to deterioration in tensile properties [3,4]. The application of RIPS to prepare sub-micron TPVs with limited rubber connectivity may be achieved by changing the cross-linking chemistry and, thus, the gelation kinetics and phase separation behavior.

Acknowledgement

This work is part of the Research Programme of the Dutch Polymer Institute (DPI) under project number 537.

References

[1] Coran AY. In: Holden G, Legge NR, Quirk R, editors. Thermoplastic elastomers. Munich: Hanser; 2004 [chapter 7].
[2] De SK, Bhowmick AK. Thermoplastic elastomers from rubber–plastic blends. New York: Ellis Horwood; 1990.
[3] Coran AY, Patel R. Rubber Chem Technol 1980;53:141–50.
[4] Araghi HH. Proceedings of the international rubber conference, Birmingham; 2001.
[5] Li Y, Oono Y, Kadowaki Y, Inoue T, Nakayama K, Shimizu H. Macromolecules 2006;39:4195–201.
[6] l'Abee RMA, Goossens JGP, van Duin M. Rubber Chem Technol 2007;80:311–23.
[7] Sultan J, McGarry FJ. Polym Eng Sci 1973;13:29–34.
[8] Verchère D, Pascault JP, Sautereau H, Moschiar SM, Riccardi CC, Williams RJJ. J Appl Polym Sci 1990;41:467–85.
[9] Verchère D, Pascault JP, Sautereau H, Moschiar SM, Riccardi CC, Williams RJJ. J Appl Polym Sci 1991;42:701–16.
[10] Moschiar SM, Riccardi CC, Williams RJJ, Verchère D, Sautereau H, Pascault JP. J Appl Polym Sci 1991;42:717–35.
[11] Verchère D, Pascault JP, Sautereau H, Moschiar SM, Riccardi CC, Williams RJJ. J Appl Polym Sci 1991;43:293–304.
[12] Bucknall CB, Partridge IK. Polymer 1983;24:639–44.
[13] Bucknall CB, Gilbert AH. Polymer 1989;30:213–7.
[14] Pearson RA, Yee AF. J Appl Polym Sci 1993;48:1051–60.
[15] Meijer HEH, Venderbosch RW, Goossens JGP, Lemstra PJ. High Perform Polym 1996;8:133–67.
[16] Ishii Y, Ryan AJ. Macromolecules 2000;33:158–66.
[17] Chen J, Chang F. Macromolecules 1999;32:5348–56.
[18] Chen J, Chang F. Polymer 2001;42:2193–9.
[19] Chen J, Chang F. J Appl Polym Sci 2003;89:3107–14.
[20] Vanden Poel G, Goossens S, Goderis B, Groeninckx G. Polymer 2005;46:10758–71.
[21] Remiro PM, Cortazar MM, Calahorra ME, Calafel MM. Macromol Chem Phys 2001;202:1077–88.
[22] Guo Q, Groeninckx G. Polymer 2001;42:8647–55.
[23] Ratna D. Polymer 2001;42:4209–18.
[24] Prusty M, Keestra BJ, Goossens JGP, Anderson PD. Chem Eng Sci 2007;62:1825–37.
[25] Keenan MR. J Appl Polym Sci 1987;33:1725–34.
[26] Wissanrakit G, Gillham JK. J Appl Polym Sci 1990;41:2885–929.
[27] Vyazovkin S, Sbirrazzouli N. Macromol Chem Phys 1999;200:2294–303.
[28] Riccardi CC, Adabbo HE, Williams RJJ. J Appl Polym Sci 1984;29:2481–92.
[29] Kim M, Kim W, Choe Y, Park J, Park I. Polym Int 2002;51:1353–60.
[30] Vanden Poel G. PhD Thesis, Catholic University Leuven, Leuven, Belgium; 2003.
[31] Bonnet A, Pascault JP, Sautereau H, Taha M. Macromolecules 1999;32:8517–23.
[32] Macosko CW, Miller DR. Macromolecules 1976;9:199–206.
[33] Miller DR, Macosko CW. Macromolecules 1976;9:206–11.

[34] Yamanaka K, Inoue T. Polymer 1989;30:662–7.
[35] Girard-Reydet E, Sautereau H, Pascault JP, Keates P, Navard P, Thollet G, et al. Polymer 1998;39:2269–80.
[36] Inoue T. Prog Polym Sci 1995;20:119–53.
[37] Yamanaka K, Inoue T. J Mater Sci 1990;25:241–5.
[38] Verchère D, Sautereau H, Pascault JP, Moschiar SM, Riccardi CC, Williams RJJ. Rubber-toughened plastics, Advances in chemistry series. Washington, DC: American Chemical Society; 1993. p. 335.
[39] Yamanaka K, Takagi Y, Inoue T. Polymer 1989;60:1839–44.
[40] Williams RJJ, Rozenberg BA, Pascault JP. Adv Polym Sci 1997;128: 95–156.
[41] Gunton JD, San Miguel M, Sahni PS. In: Domb C, Lebowitz JL, editors. Phase transitions and critical phenomena. London: Academic; 1983. p. 269.
[42] Zheng Q, Peng M, Song Y, Zhao T. Macromolecules 2001;34:8483–9.
[43] Siggia ED. Phys Rev A 1979;20:595–605.
[44] Kim BS, Chiba T, Inoue T. Polymer 1995;36:67–71.
[45] Williams ML, Landel RF, Ferry JD. J Am Chem Soc 1955;77:3701.
[46] Tanaka H. Macromolecules 1992;25:6377–80.
[47] Tanaka H. Phys Rev Lett 1993;71:3158–64.
[48] Tanaka H. Phys Rev Lett 1996;76:787–90.
[49] Gan W, Yu Y, Wang M, Tao Q, Li S. Macromolecules 2003;36:7746–51.
[50] Ishii Y, Ryan AJ. Macromolecules 2000;33:167–76.